PROCEEDINGS OF THE HSD STUDENT ENGINEERING CONFERENCES

Selected Papers from the Courses 2018/2019 | Issue 1

ISSN 2700-1857

Preface

With the completion of their bachelor thesis, engineering students have usually carried out and compiled a genuine piece of research. However, even with a thorough supervision, the exposition of results and arguments often remains limited to a small internal circle of stakeholders in a protected research environment and/or in an examination process. The students therefore miss the learning experience of being challenged by a broader audience of experts and peers. Such an advance into new and open terrain may look like trouble ahead for our students but is often the doorstep to new advances in learning.

At an institutional level, various approaches to learn and train the written and oral presentation of scientific work can be found. Commonly, the required skills of students are developed throughout continuous assignments to write lab reports, project documentations and, finally, the bachelor thesis. Ideally, the student develops her/his own style and skills with respect to authorship by learning from various staff members, but the learning process is rarely made explicit or guided. On the contrary, ambitious and valuable courses like "Writing your thesis" or "Presentations for engineers" exist, but are often offered on a voluntary basis and/or outside the faculty. This can convey misleading messages with respect to developing a self-confident authorship. It implies that communication and presentation is only an add-on for either those with special weaknesses or special interests and may thus remain detached from the development of the student's identity as an engineer.

"Engineering Conferences" was established as a course for master's students to increase the scientific literacy of our future engineers. It is a mandatory part of the curriculum at the Faculty of Mechanical and Process Engineering of the Düsseldorf University of Applied Sciences. The intention of designing Engineering Conferences as a teaching unit was to improve professional communication skills, to increase the visibility of undergraduate research and to make engineering research an integral part of the curriculum. By using the bachelor thesis as a starting point, a scientific paper and poster are developed by each student in the course. The course follows the schedule of typical engineering conferences, including a full peer-review process, the use of conference organising tools and a public poster presentation in the end.

Since its launch in 2016, the editors of this volume have been involved in the development, teaching, and examining of the course Engineering Conferences. Every term, about 30 papers and posters are submitted by the students and assessed by the teaching team. Almost all papers show a reasonable quality of scientific writing although most students did not write a report or article in the English language before. Regularly, some papers are of exceptional quality, similar or beyond to what is typically presented at real conferences in the field of engineering. With this series of conference proceedings, the best papers

submitted in partial fulfilment of the examination requirements of the course Engineering Conferences are given the chance to become real publications.

For this volume, a number of the best student papers from the courses of 2019 and 2020 were selected for a possible publication. The papers were reviewed by the editors in a process separate from the course examinations. The students were asked to rework and resubmit their papers based on the reviews by the editors. For the final version of the papers, the students were free to decide that their thesis supervisors should become additional authors.

March 2020

Matthias Neef
Thomas Zielke
Claudia Fussenecker
Jörg Niemann

Table of Contents

The Potential of Acoustic Sensors to Foster the Ecological Sustainability of a City: A Case Study in Medellin

David Duque [1], Stefanie Dederichs, and Medzid Muhasilovic [2]

[1] M.Sc. student, Düsseldorf University of Applied Sciences, Germany
david.duque@study.hs-duesseldorf.de

[2] Free University of Bolzano, Bolzano, Italy

Abstract. This research evaluates how the employment of acoustic sensors can improve the environmental conditions in Medellin, Colombia. Medellin, the second-largest city in the country, reported alarming measurements of environmental figures including air pollution, traffic noise, and forest fires. To face these problems, four different acoustic sensing applications were discussed with experts from technical, social, and legal branches to evaluate their feasibility. Furthermore, a spectral analysis was conducted to trace the frequency range of sound events in outdoor environments. Acoustic sensors can be integrated as a tool for monitoring vehicle traffic. They can also be embedded in video-based systems to penalize vehicles that surpass the permitted sound emission level limits. Moreover, acoustic sensors can help to react against forest fires in sensor-fusion with temperature and smoke sensors, and as an early warning system, could recognize animal reactions to environmental phenomena. The results represent a theoretical framework. Therefore, further research in each of the example cases is encouraged.
Keywords: Passive acoustic sensors, ecological sustainability, smart cities, environmental pollution.

1 Introduction

In recent years, Medellin has reported alarming statistics about its environmental situation. Regarding air particle pollutants, it was found in 2016 that the average particle pollution value which is smaller than 2,5µm ($PM_{2,5}$), surpassed the limit established by the Colombian norm [1] of 25µg/m^3 at nine out of eleven measuring stations. Traffic noise is another concern. According to the values given in Medellin's 2016 environmental report [2], 100% of the daily and nightly median values surpassed the established limits given by the Colombian resolution of permitted noise emissions [3].
Moreover, forest fires are an important cause of deforestation in Medellin and the whole department of Antioquia and a factor that negatively affects the air quality. It was probed that they release particle pollutants like $PM_{2,5}$ into the atmosphere [4].

Due to new technological developments in networks, sensors, and machine learning, the concept of smart cities has increasingly gained interest in research communities [5]. New research has shown that acoustic sensors can be used for applications that could be used to monitor sound events in cities and their surroundings (see section 2).

This paper focuses restrictedly on passive acoustic sensors detecting frequencies within the human hearing range, leaving infrasound and ultrasonic waves to future research. Likewise, this research only considers waves that propagate through the air. Hence, acoustic sensors that work in other propagation media such as water, or mechanical vibrations that spread out through solids are out of the scope of this project.

A technological assessment was done by interviewing experts from data science, acoustic monitoring, acoustic sensors, environmental noise, social, and legal branches. These experts evaluated how different applications could be used to improve traffic by monitoring it; to reduce sound levels by creating a penalization system; to optimize car park energy consumption by monitoring automobile sound emissions; and by eventually recognizing forest fires.

Afterward, an experiment was conducted to extract the frequency content of audio samples taken in outdoor environments. It was carried out to establish the frequency ranges of different sound events that are applicable to the four example cases.

2 Acoustic Sensing in Smart Cities

During the last years, there have been innovative improvements in acoustic sensing technology. Some of the applications in the field of acoustic monitoring and sound recognition are presented here.

Acoustic sensors were installed in strategic street crossings to detect ambulances approaching the streetlights, which connected to the acoustic monitoring system, prioritize the ambulance traffic. The project is called EAR-IT and was supported by the European Union [6].

Nirjon et al. [7] performed an analysis of audio samples recorded with smartphones in a building. Then, to evaluate the data, they generated spectrograms to be able to predict malfunctions in *Heat, Ventilation and Air-conditioning Systems* (HVAC). To model and encode the regular pattern of the acoustic time series data of an HVAC running system, they used an unsupervised learning approach by applying machine learning algorithms. In the experiment, they identified regular patterns of the signal and assessed if the systems deviate from the regular patterns to later predict possible issues.

Uziel et al. [8] and Ehrig & Hollosi [9] developed projects to improve energy consumption by estimating the occupancy rate in buildings and their surroundings. As a result, they pursued to eliminate the unnecessary consumption of energy without affecting the well-being or privacy of the building´s visitors. For the process, they used acoustic localization algorithms to generate acoustic maps, and machine learning algorithms to recognize occupancy levels by analyzing recorded audio samples [9].

The past examples show how acoustic sensors have been used to monitor sound events. In this paper, the research focusses beyond the multiple applications on smart

environments and induces new possibilities to focus these technologies for the sake of improving concrete environmental problems.

3 Expert Interviews: Method and Results

Three experts from the technical fields of acoustic monitoring, technology management, and computer science were interviewed to investigate technical solutions of acoustic monitoring in the scenarios described in section 1. Three further experts in environmental noise, social and legal branches provided comprehensive input regarding the deployment of new projects in the city. The expert interviews were transcribed and evaluated following the interview analysis method by Mühlfeld et al. [10] cited in Mayer [11]. The results of the interviews are summarized in the next sub-sections:

3.1 Vehicle Traffic Monitoring

Traffic can be measured to provide a city with intelligent solutions and improve its traffic overloading. One way of measuring traffic is to place an array of two microphones, looking at the audio waves emitted by the cars at two checkpoints, and finally by using cross-correlation methods to find the time onset of the cars. This will give valuable information related to the traffic flow. The operating model is shown in Fig. 1.

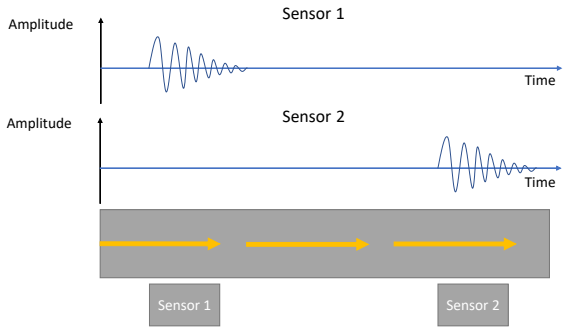

Fig. 1. Model of the Vehicle Traffic Monitoring System (Source: Expert 1)

As an automobile passes through the checkpoints, the time is recorded and its onset is computed by the microprocessor giving an estimation of the speed of the vehicle.

3.2 Traffic Noise Monitoring

A traffic noise monitoring application, operating in conjunction with the flashing cameras functioning in the city, would trigger a fine once the permitted sound level in the area is violated. Noise is usually measured using the *root mean squared* (RMS), which is the average sound pressure of a signal. It is done by summing up all the squared

pressure levels and taking the square root of this sum. To convert to decibel, the logarithm of the RMS multiplied by twenty is computed. Every microcontroller can execute this operation. In this situation, it is important to filter unwanted signals and work with measurements of small timeframes to retrieve accurate information from the system. The compatibility of the embedded video and audio equipment, as well as the microcontroller's processor and other electronic gear, must be ensured. Additionally, the system should be vandalism and weatherproof. Real-time processing is required, thus a microprocessing unit with a Cortex A8 core will suffice for sound monitoring based on previous research [12].

3.3 Car Parks Monitoring

A deployment of acoustic sensors to monitor car occupancy rates in car parks and linked to their HVAC system to improve the indoor air quality while optimizing energy consumption is, at first sight, expensive and even unnecessary. Furthermore, from the legal aspect, the installation of an acoustic-based system inside a car park is ethically debatable, since human voices are more likely to be recognized. Therefore, the privacy of the visitors could be violated [1].

An eventual sound monitoring application linked to the HVAC system can be outperformed by a such that uses the entry barriers of the car parks to monitor its occupancy rate, fulfilling this function. Though having an acoustic-based system that is capable of monitoring other events, as already described in section 1, could improve the capability to detect occupancy rates in buildings and also prevent failures in the HVAC equipment, as stated in the literature [7].

3.4 Forest Fires Monitoring

Either a linear array or a triangular array placed at the perimeter of the forest with acoustic sensors can be deployed to monitor sound activities in forests. Though, it is difficult to find forest fire's audio training material for machine learning purposes. Additionally, a poor accuracy related to the audio recognition of the fires is expected. Therefore, other kinds of sensors need to be deployed in the system. As an alternative, by fusing the microphone arrays with off-the-shelf temperature and smoke sensors placed at equal distances and covering the area of the forest. The frequency response of the acoustic sensors needs to cover the presence and treble frequency ranges (see Table 1) since these alarms emit sounds at about at 3000 Hz [2]. Acoustic sensors can be further utilized to monitor animal activity and use this data for early warning purposes (see also [15]). For this system, a housing that is robust, i.e., weather and vandalism proof is required. The temperature sensors also require additional protection. In contrast to the acoustic monitoring system, a set of smoke or temperature sensors

[1] There are methods to evaluate the presence of human voice in audio samples. See also [13] & [14].

[2] Two samples of different fire alarms were recorded by the author and the frequency content was extracted and analyzed with *MATLAB* retrieving this value.

with their own transceivers and connected either via Wi-Fi in a peer-to-peer base or GSM network, do not allow the chance to monitor wildfire sound events.

4 Acoustic Spectral Analysis: Method and Results

To identify frequency ranges where sound events were particularly present and to recognize the adequate microphone´s frequency response for each of the studied cases, 24 samples were recorded in outdoor environments followed by an analysis of the digitalized acoustic signals. Additionally, the performance of two different microphones, which also have different filtering characteristics and sound quality, was compared.

The recordings were made using a *Sony IC Recorder ICD-PX720* at super high-quality recording (frequency range 75 Hz to 20 kHz) and sensitivity set to high[3]. Besides, a cellphone *Huawei Honor 8* which has a dynamic microphone [16] with noise-canceling technology was used. Finally, the samples were analyzed with *MATLAB R2017B*. The analysis was done using a slightly modified script [17] to spot acoustic relevant events and trace their sound frequency ranges. Examples of the spectral analysis can be found in figures 2 and 3.

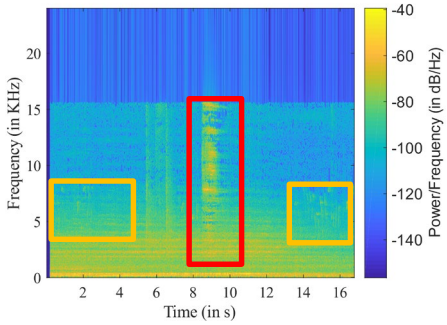

Fig. 2. Spectrogram - Honor 8 Recording #12 (birds within yellow squares, train within red square)

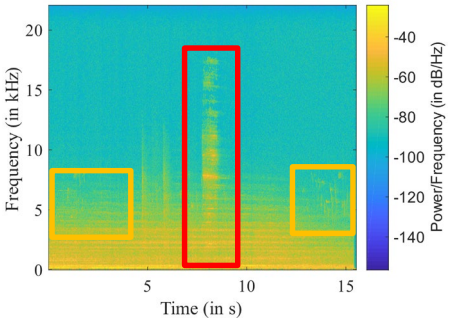

Fig. 3. Spectrogram - Sony Voice Recorder Recording #12 (birds within yellow squares, train within red square)

In the spectrograms above, birds singing (at t= 0-4 s and t=14-16 s) on the frequencies between 5 kHz to 8 kHz, and a train passing (at t= 9 s) on the frequencies up to 18 kHz were detected. The Honor 8 microphone did not recognize the whole signal spectrum of the train since it filters out frequencies above 15 kHz (see dark blue area of the spectrogram in Fig. 2). Moreover, the filter is not only designed to limit high frequencies but also to smooth sound levels (see blurred areas specially in the presence and treble ranges). The Sony Voice Recorder captured the whole spectrum and there is not any recognizable filter on the signal (see Fig. 3).

[3] There is no reference to the microphone type on the product specifications.

In summary, the microphones for traffic monitoring could provide a better output with a frequency response between the *bass* frequencies until the *presence range*, since from the spectral analysis, in this range most of the vehicle traffic activity was captured. For forest monitoring cases, an emphasis on the *presence range* might help to recognize the fire alarms and fauna activity, whereas sensible condenser super-cardioid microphones [18] with a sound filtering layer are required to retrieve an accurate signal. For sound level measurement cases, a measurement microphone sensitive to frequencies from the *sub-bass range* up to the *treble range* might be reasonable since one of the audio samples of a double-cabin bus covered frequencies up to 18 kHz. The following table illustrates the sound frequency ranges:

Table 1. Characterization of Frequency Ranges (Source: [19])

Frequency Subrange (Hz)	Characterization
40	Sub Bass
40-200	Bass
200-500	Low Middles
500-3,000	Middle Range
3,000-7,000	Presence
7,000-14,000	Treble
>14,000	Air Band

5 Discussion and Future Research

Although the actual environmental situation in Medellin is very critical and the administration has put effort into improving, measuring and reporting of problems, there is not any research to be found in the field of acoustic sensing to improve the mentioned ecological aspects of the city.

The presented approach to face different kinds of ecological problems can support to improve environmental conditions in any city by monitoring them. Nevertheless, there are uncountable other factors that affect the city's environmental situation, e.g., the ethics of managing the traffic monitoring system. It is also crucial to bear in mind that acoustic monitoring should filter out human voices to protect people´s privacy. Hence, the data needs to be secured against misuses and possible exposure to malware.

Acoustic sensors and acoustic monitoring possess a vast potential to foster the ecological sustainability of cities. This depends on the geographical location and problems related to the city's culture, and on the willingness of its administration to look for innovative technologies. Nonetheless, the price-performance ratio of the sensors can be exploited at its maximum when different sound monitoring modalities are utilized with the same *Acoustic Processing Unit*.

The experiment's hypothesis lies on the premise that microphones with a frequency response emphasizing the range similar to the acoustic events could improve the sound recognition. This premise must be investigated in the future with practical experiments. Future research should additionally delve into the following aspects: decision on the exact product specifications related to microphones and their components, the exact

configuration and procedures to conduct a real-time sound recognition, as well as the settings of the microphone arrays to retrieve reliable results.

References

1. Resolución 610 del 24 de Marzo de 2010 “Calidad del Aire” (Resolution 610 by the 24th of march, 2010 “Air Quality”), http://www.minambiente.gov.co/images/normativa/app/resoluciones/bf-Resoluci%C3%B3n%20610%20de%202010%20-%20Calidad%20del%20Aire.pdf, (2010).
2. Estado de los Recursos Naturales y del Medio Ambiente 2016 - Municipio de Medellin (Status of Natural and Environmental Resources - Medellín City). Contraloria General de Medellín, Medellín (2017).
3. Colombian Environmental Ministry: Resolución 0627 de 2006: por la cual se establece la norma nacional de emisión de ruido y ruido ambiental. (Resolution 0627 of 2006: to stablish national noise emission limits and environmental noise limits), http://www.alcaldiabogota.gov.co/sisjur/normas/Norma1.jsp?i=19982, (2006).
4. Chen, M., Gu, Y., Liu, M., Li, J.: Estimating PM 2.5 in British Columbia Before and After Wildfires using 3 KM Modis AOD Products from February to August 2017. In: IGARSS 2018 - 2018 IEEE International Geoscience and Remote Sensing Symposium. pp. 7585–7588. IEEE, Valencia (2018). https://doi.org/10.1109/IGARSS.2018.8517475.
5. Hancke, G.P., de Carvalho e Silva, B., Hancke, G.P.: The Role of Advanced Sensing in Smart Cities. Sensors. 13, 393–425 (2012). https://doi.org/10.3390/s130100393.
6. In the smart city of Santander, the walls have ears, http://www.euronews.com/2014/10/13/in-the-smart-city-of-santander-the-walls-have-ears, (2014).
7. Nirjon, S., Srinivasan, R., Sookoor, T.: Smart Audio Sensing-Based HVAC Monitoring. In: Smart Cities: Foundations, Principles, and Applications. pp. 669–695. Wiley, Hoboken, NJ (2017).
8. Uziel, S., Elste, T., Kattanek, W., Hollosi, D., Gerlach, S., Goetze, S.: Networked embedded acoustic processing system for smart building applications. In: Design and Architectures for Signal and Image Processing (DASIP), 2013 Conference on. pp. 349–350. IEEE (2013).
9. Ehrig, L., Hollosi, D.: The Last One Out Turns off the Light - Optimizing the Energy Efficiency of Buildings, https://ercim-news.ercim.eu/en92/special/the-last-one-out-turns-off-the-light-optimizing-the-energy-efficiency-of-buildings.
10. Mühlfeld, C., Windolf, P., Lampert, N., Krüger, H.: Auswertungsprobleme offener Interviews. Soz. Welt. 32, 325–352 (1981).
11. Mayer, H.O.: Interview und schriftliche Befragung: Grundlagen und Methoden empirischer Sozialforschung. Oldenbourg Verlag, München (2013).

12. Hollosi, D., Nagy, G., Rodigast, R., Goetze, S., Cousin, P.: Enhancing Wireless Sensor Networks with Acoustic Sensing Technology: Use Cases, Applications amp; Experiments. In: 2013 IEEE International Conference on Green Computing and Communications and IEEE Internet of Things and IEEE Cyber, Physical and Social Computing. pp. 335–342 (2013). https://doi.org/10.1109/GreenCom-iThings-CPSCom.2013.75.
13. Ali, Z., Talha, M.: Innovative Method for Unsupervised Voice Activity Detection and Classification of Audio Segments. IEEE Access. 6, 15494–15504 (2018). https://doi.org/10.1109/ACCESS.2018.2805845.
14. Zgank, A.: Acoustic Monitoring and Classification of Bee Swarm Activity Using MFCC Feature Extraction and HMM Acoustic Modeling. In: 2018 ELEKTRO. pp. 1–4. IEEE, Mikulov (2018). https://doi.org/10.1109/ELEKTRO.2018.8398253.
15. Stowell, D., Benetos, E., Gill, L.F.: On-Bird Sound Recordings: Automatic Acoustic Recognition of Activities and Contexts. IEEEACM Trans. Audio Speech Lang. Process. 25, 1193–1206 (2017). https://doi.org/10.1109/TASLP.2017.2690565.
16. Akino, H.: Dynamic Microphone, http://www.freepatentsonline.com/8098871.html, (2012).
17. Zhivomirov, H.: Sound Analysis with MATLAB Implementation - File Exchange - MATLAB Central, http://de.mathworks.com/matlabcentral/fileexchange/38837-sound-analysis-with-matlab-implementation.
18. Akino, H.: Condenser Microphone, http://www.freepatentsonline.com/y2006/0251274.html, (2006).
19. How Frequency Response Helps You to Understand the Sound of a Microphone, http://www.neumann.com/homestudio/en/how-does-frequency-response-relate-to-sound.

Aerodynamic Analysis of Passenger Car Cooling-Fan-Modules with Varying Strut Configurations on a Modular Chamber Test Rig

Marvin Fritsche [1] and Igor Neifach

[1] M.Sc. student, Düsseldorf University of Applied Sciences, Germany
marvin.fritsche@study.hs-duesseldorf.de

Abstract. This paper deals with the aerodynamic analysis of passenger car cooling-fan-modules with varying downstream strut configurations on a specially developed modular chamber test bench. The concept for the test bench is verified by a Computational Fluid Dynamics (CFD) simulation and then put into practice. Various strut configurations have been tested with regard to their aerodynamics using the developed test bench. The main goal was to compare an acoustically preoptimized strut configuration to a commercial serial configuration.
In the course of the investigation, it was determined that specific design parameter changes have a significant influence on aerodynamic performance. Changes in the volume flow rate of up to 8%, the differential pressure of up to 12.6% and the aerodynamic efficiency of up to 2.2% were observed. A direct correlation between acoustic and aerodynamic performance has also been found.

Keywords aerodynamic performance, struts, axial fan, rotor-stator interaction

1 Introduction

Based on the results of aeroacoustic investigations within the research group, several strut configurations have been selected for this work in order to investigate them aerodynamically [1]/ [2].

In the automotive sector, the cooling of an internal combustion engine or the battery packs of an electric motor is carried out using cooling fan modules (CFM). Cooling is mainly achieved by convective heat transfer to an air stream flowing through a heat exchanger. Particularly in parking situations, the CFM is essential to maintain the required air flow. Sufficient aerodynamic performance of the CFM is essential to maintain this flow rate necessary for cooling. In numerous investigations, the rotor blades of various fans were analyzed and optimized so that complex designs were created. But most research is focused on acoustic optimization of the rotor blade shape, see e.g. the work of T.Biedermann et al. [3], J.-H. Kim et al. [4] and G.Angelini [5]. The rotor-stator interaction is far less part of the research.

As Neifach et al. [1] demonstrated, rotor-stator interaction has a great potential with regard to acoustic optimization. In order to satisfy the high requirements of cooling fan

modules, it is necessary to investigate the aerodynamic characteristics of the acoustically optimized struts. In his research, Neifach was able to develop acoustically optimized struts for a forward swept, unevenly spaced axial fan [2]. The aim of the current study is to investigate possible aerodynamic drawbacks due to the rigorous changes in the strut configuration. For the aerodynamic investigations, a suction side chamber test bench has been combined with the specially developed acoustic test bench. A CFD simulation was carried out to validate the test bench concept.

In the following the resulting possibilities, which seem to offer the greatest optimization potential, are summarized. Although it is possible to reduce noise emissions by maintaining the longest possible distance between rotor and stator, this usually cannot be achieved in practice due to space restrictions. However, by leaning the struts in the circumferential direction, noise emission can be reduced, even if the installation space is limited. Bending in the circumferential direction can also lead to a reduction in noise emissions. Modifications to the cross-sectional shape of the struts also show a promising approach to reducing noise emissions. Furthermore, the number of struts should be selected in a way that there are no common divisors between the rotor and stator blade numbers. Even by varying the angle of attack of the struts over the circumference, rotor vibrations could be reduced [1].

2 The CFM Parameters

A fan with nine forward curved, unevenly arranged blades was used for the investigations. In the series module six unevenly arranged struts are installed, which are leaned against the direction of fan rotation. The figures 1 and 2 illustrate the design and installation of the CFM.

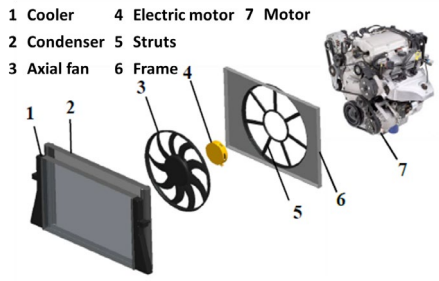

Fig. 1. Exploded view of the CFM [2]

Fig. 2. Fan with frame

Table 1 shows an overview of the most important key parameters for the cooling fan module.

Table 1: Basic data of the CFM [1]

Number of fan blades	9	[-]	Number of struts	6	[-]
Fan hub diameter	170	[mm]	Strut width	18	[mm]
External fan diameter	445	[mm]	Strut depth	17	[mm]
Rotational speed	2700	[rpm]	Blade to strut clearance at the hub	12	[mm]
Blade tip mach-number	0.35	[-]			

3 Experimental Setup

An existing CFM test bench from the Institute of Sound and Vibration Engineering (ISAVE) at the University of Applied Sciences Düsseldorf has been modified in order to be coupled to a suction side chamber test bench (DIN EN ISO 5801). This test bench allows various strut configurations to be easily exchanged and measured. The following Fig. 3 shows the structure of the created test bench.

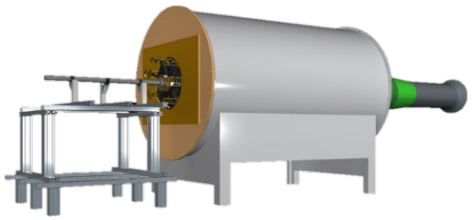

Fig. 3. Aerodynamic test bench

The modular design of the test bench allows the quick variation of the struts and their degrees of freedom, as well as the exchange of the CFM. For the pressure measurement, static pressure probes were used, which were equally distributed over the cross-section of the chamber and the nozzle.

3.1 Measured strut configurations

In order to gain insight into the fundamental effects of the strut shapes, the configurations "straight round" and "bend lean round" as well as "strut-free" (see Fig. 4) were measured in addition to the acoustic optimum and the series module. The acoustic optimum found by Neifach [1] shows a 17 dB(A) lower sound pressure level for the blade passage frequency tone and a 2.6 dB(A) lower overall sound pressure level than the state-of-the-art industrial series module. The series module is used as the baseline for the investigations, which are compared with the aerodynamic performance of the acoustic optimum. Since lean and bend of the struts had the most significant effect on acoustics in Neifach's investigations, these configurations were also evaluated with respect to aerodynamic performance. As a reference, the cooling fan module was measured without struts.

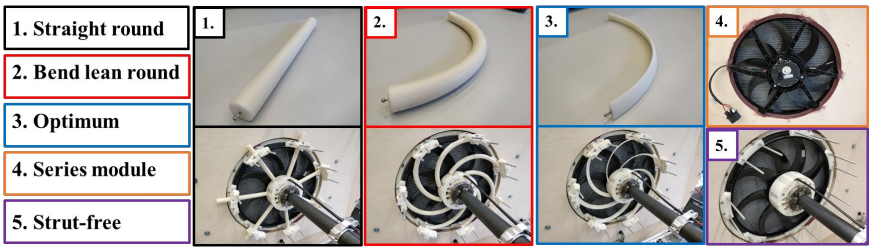

Fig. 4. Variation of the strut configurations and shape of the struts

4 CFD simulation

A CFD simulation was performed to check whether the test bench is suitable for the selected measurement technique or not. To ensure a valid pressure measurement, the trajectories around the measuring position must be straight and the velocity must be under 1 m/s.

Fig. **5** shows the course of the streamlines in a steady state case and the velocity in the longitudinal section of the test bench. Fig. 6 shows a contour plot on the position of the pressure probes. It becomes clear that the flow velocities are all well below 1 m/s and thus a static pressure measurement can be carried out. The simulation results also showed no unwanted backflow areas or flow detachment, so that the test bench concept was implemented according to plan.

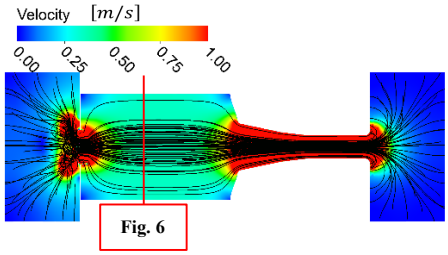

Fig. 5. Speed contour with streamlines in the longitudinal section of the test bench

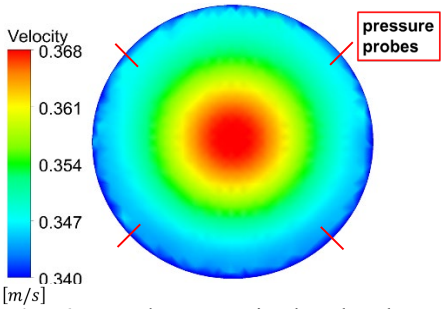

Fig. 6. Speed contour in the chamber at the height of the static pressure probes

5 Methodology

Here the basic calculations used for the evaluation of the measurement data are described. In the following, the values are denoted by indices, where the index "ch" stands for chamber and the index "n" for nozzle.

To determine the density ρ, the thermal equation of state of ideal gases (1) is resolved with respect to ρ and the measurement data for temperature T and pressure p, as well as the specific gas constant R are used. For the low velocities of this investigation, the flow can be regarded as incompressible and thus, a single density for the whole test rig

including the CFM can be used. The required temperature measurement was performed by using a temperature dependent resistance PT1000 inside the chamber.

$$\rho = \frac{p_{ch}}{R \cdot T_{ch}} \tag{1}$$

The flow velocity is calculated based on the Bernoulli equation.

$$\frac{c_\infty^2}{2} + \frac{p_\infty}{\rho} + z_\infty \cdot g = \frac{c_n^2}{2} + \frac{p_n}{\rho} + z_n \cdot g \tag{2}$$

With the assumptions $z_\infty = z_n$, $c_\infty = 0$ and $\rho = constant$, the Bernoulli equation can be simplified accordingly. This case-related equation can be solved according to c_n .

$$c_n = \sqrt{\frac{2 \cdot p_n - p_\infty}{\rho}} = \sqrt{\frac{2 \cdot \Delta p_n}{\rho}} \tag{3}$$

The volume flow is calculated using equation (4). The α-value is an empirically determined correction factor for the corresponding nozzle. In this work, an α-value of $\alpha =$ 0,98 was used, based on fluidic tests in the laboratory of the University of Applied Sciences Düsseldorf.

$$\dot{V} = \alpha \cdot c_n \cdot A_n \tag{4}$$

The specific work of a fan describes the specific energy difference between the suction and discharge nozzles of the turbomachine [6]. Under the assumptions already made, the specific nozzle work can be determined according to

$$Y = \frac{\Delta p_{ch}}{\rho} + \frac{c_{ch}^2}{2} \tag{5}$$

The effective aerodynamic performance can be determined by the product of the mass flow and the specific nozzle work. The mass flow is calculated by multiplying the volume flow by the density of the medium.

$$P_{aero} = \dot{m} \cdot Y = \dot{V} \cdot \rho \cdot Y \tag{6}$$

The division of the aerodynamic power P_{aero} by the drive power P_{drive} results in the aerodynamic efficiency η_{aero}. The electrical power P_{el} must be multiplied by the efficiency of the motor η_{system} to determine the actual drive power P_{drive}.

$$\eta_{aero} = \frac{P_{aero}}{P_{drive}} = \frac{P_{aero}}{\eta_{system} \cdot P_{el}} \tag{7}$$

The flow coefficient is a dimensionless characteristic value for describing the throughput of turbomachinery. It is calculated from the volume flow, the rotational speed and the impeller area.

$$\varphi = \frac{4 \cdot \dot{V}}{\pi^2 \cdot D^3 \cdot n} \tag{8}$$

6 Results

The staggering of the determined characteristic curves for the individual configurations in the different representations show a similar behaviour throughout (see Fig. 7). The acoustic optimum (blue) shows the best aerodynamic performance of the measured strut configurations especially in the range of the flow coefficient φ = 0,03 – 0,07. In this range, the acoustic optimum delivers for some points even a higher aerodynamic performance than the strut-free configuration. A possible explanation for this behavior could be, that the struts provide an improved flow guidance and thus convert additional energy from the curling motion to additional pressure rise. Compared to the series module as the baseline, all configurations attain a significantly higher aerodynamic efficiency.

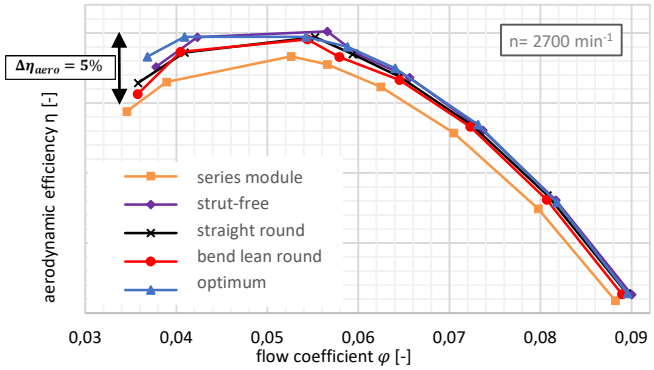

Fig. 7. Aerodynamic efficiency over flow coefficient for various strut configurations

Fig. 8 also shows that the design parameters of bend and lean have little effect on aerodynamics compared to the acoustic results from the previous investigations [1]. A slightly lower volume flow as a result of leaning and bending tend to be derived. This behavior can be explained by a larger blocked area of the leaned and curved struts in the direction of flow. This marginal disadvantage of inclination and curvature, however, can almost be solved by a skillful shaping of the strut cross-section, as shown by the good aerodynamic performance of the variant “acoustic optimum”.

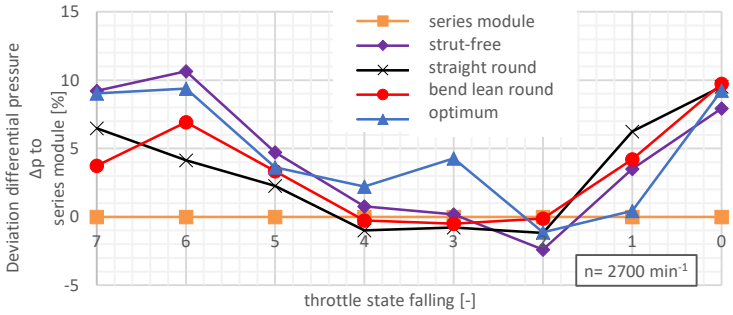

Fig. 8. Percentage deviation of differential pressure to series module

7 Conclusion

The evaluation of the investigation shows that the acoustic optimization approaches have generally a positive effect on the aerodynamic performance of the strut configurations compared to a standard module. For most of the aerodynamic characteristics, a significant improvement could be achieved compared to the standard module. The acoustic optimum determined within the framework of the previous investigation generally also exhibits the best aerodynamic performance [1]. Compared to the standard module, the strut variant “acoustic optimum” can generate up to 8% higher volume flow and up to 9.4% higher differential pressure. The aerodynamic efficiency is up to 1.4% higher than that of the standard module.

With this work it was shown that the aerodynamic efficiency of radiator fan struts is dependent on their cross-sectional shape. The skillful design of the strut cross-section allows to create a guiding effect, which converts additional energy from the curling motion into additional pressure rise. In addition, it was shown that the influence of bend and lean, in contrast to acoustics, is rather insignificant to the aerodynamic performance [1].

Acknowledgments.
The work reported in this paper was supported by the Brose Fahrzeugteile GmbH, Oldenburg.

References

1. I.Neifach, Aeroacoustic optimization of a preasure-side strut configuration for subsonic axial fans using statistical-empirical modelling, Oslo, Norway: ASME 2018 Turbo Expo, (2018).
2. I. Neifach, Aeroakustische Optimierung einer druckseitig angeordneten Strebenkonfiguration bei axialen Niederdruckventilatoren in PKW-Kühlerlüftermodulen, Düsseldorf: Hochschule Düsseldorf, (2017).
3. T. Biedermann, T. P. Chong und F. Kameier, Statistical-empirical modelling of aerofoil noise subjected to leading edge serrations and aerodynamic identifica-tion of noise reduction mechanisms., Lyon, France: 22nd AIAA/CEAS Aeroacoustics Confer-ence, (2016).
4. J.-H. Kim, J.-H. Choi, A. Husain und K.-Y. Kim, Performance enhancement of axial fan blade through multi-objective optimization techniques, Rep. of Korea : Springer: Journal of Mechanical Science and Technology , (2010).
5. G. Angelini, T. Bonanni, A. Corsini, G. Delibra, L. Tieghi und D. Volponi, Optimization of an axial fan for air cooled condensers, Rome, Italy: Elsevier: Energy Procedia, (2017).

6. G. Na, Numerical simulations of unsteady aerodynamic effects in the blade tip region of cooling Fans with subsequent experimental validation for the purpose of acoustical optimization, Düsseldorf: University of Applied Sciences Düsseldorf, (2015).

Performance Analysis of Biodiesel and its Blends in a Variable Compression Ratio Engine

Tarang Mehta[1], Akshay Gare[2], Manesh Sikarwar[2], Sudhin Poduval[2]

[1] M.Sc. student, Düsseldorf University of Applied Sciences, Düsseldorf, Germany
tarang.mehta@study.hs-duesseldorf.de

[2] Navrachana University, Vadodara, India

Abstract. Experiments were carried out to estimate the performance of a single cylinder, water-cooled four-stroke Variable Compression Ratio (VCR) diesel engine fuelled with palm biodiesel. A detailed comparison of the performance parameters of pure diesel and 5%, 10%, 15%, 20% blends of biodiesel were performed at a fixed compression ratio 17.5 and at different loading conditions. In this paper, the performances were checked using parameters which includes brake power, mechanical efficiency, brake thermal efficiency (BThE) and brake specific fuel consumption (BSFC). An optimal value at the compression ratio of 17.5 for the blend with maximum performance was obtained. This optimal blend was then compared with the diesel for the same parameters. The findings within this report lead to the conclusion that currently running vehicles can efficiently use blends with 20% of biodiesel at the compression ratio of 17.5.

Keywords: Biodiesel, Variable Compression Engine (VCR), Performance, brake power, Compression Ratio.

1 Introduction

The population of vehicles running on fossil fuels is still increasing each year leading to peak pollution levels. Mismatch between demand and supply of fossil fuels, fluctuating fuel prices and associated pollution problems question the existence of fossil fuels in the long run [1]. It has been found that vegetable oils are becoming a promising alternative because their properties are comparable to that of diesel and are produced from crops with minimum effort. Vegetable oils are easily available, are renewable, have a reasonably high Cetane number and can be used in diesel engines with simple modifications. They can also be easily blended with diesel in the neat and esterified (biodiesel) forms [2]. Biodiesel is produced from available resources like vegetable oils (palm, peanut, sunflower, rape, coconut, karanja, neem, cotton, Mustard, jatropha, linseed, and castor), animal fat (pork or chicken) and greases (used cooking oils) through a chemical process known as transesterification. Due to the demand of edible oil for domestic purposes, non-edible oil is preferred for biodiesel production.

Biodiesel has several advantages over fossil fuel such as smoother engine operation by enhancing better lubricating properties and better combustion characteristics. On the

opposite, it has some disadvantages, such as the higher production cost and the poor cold flow properties of biodiesel when used it in a colder climate. Biodiesel can reduce greenhouse gas emissions to the atmosphere by lowering CO, HC and particle matters, etc. Non-edible oils that can be used to produce bio-fuels are gaining worldwide acceptance as one of the comprehensive solutions for problems of environmental degradation, energy security, restricted imports (import restrictions), rural employment and agricultural economy [3].

Increasing worldwide demand for conventional fuels and reducing carbon emissions has led to significant work into improved formulations of fuel and reduced levels of smoke and particles. Nevertheless, with engine upgrades alone, it is difficult to achieve the necessary emission standards. Blending the diesel with different vegetable oils has proven to be an alternative method for achieving low emissions and better diesel combustion performance. In the last two decades, this has been the focus of most research in this field.[4]

In this study, all the experiments are performed without any hardware modification on the engine. The performance characteristics of the diesel engine are investigated by using pure diesel and the blends of palm biodiesel with diesel. The parameters which are varied during testing are load and blend at a constant compression ratio of 17.5.

2 Experimental Setup and Methodology

The present investigation was carried out on a fully computerized experimental engine test rig comprising of a single cylinder, water-cooled, and four-stroke variable compression ratio (VCR) diesel engine connected to an eddy current dynamometer for loading. The setup includes necessary instruments for the online measurement of cylinder pressure, injection pressure, and crank angle.

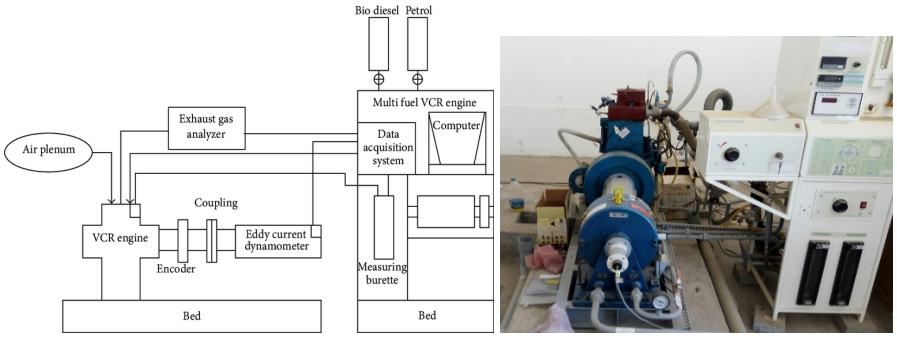

Fig. 1. Engine setup (left) [6] and experimental setup (right) of engine.

According to a conventional arrangement for changing the compression ratio as a function of operational conditions, the connecting rod of each piston is subdivided into two connecting rod parts which are coupled with one another by a central joint. [5]

The compression ratio can be changed without stopping the engine and without altering the combustion chamber geometry by a specially designed tilting cylinder block

arrangement. Continuous circulation of water is maintained for cooling the sensors and to maintain the required temperature by using a small water pump.

Readings of various parameters such as brake power, mechanical efficiency, brake specific fuel consumption, brake thermal efficiency with biodiesel for compression ratio 17.5 were collected at various loads varying from 0 to 9kg for all the blends B5 (95% diesel and 5% biodiesel), B10 (90% diesel and 10% biodiesel), B15 (85% diesel and 15% biodiesel) and B20 (80% diesel and 20% biodiesel) of the biodiesel and diesel. The optimum value from all the blends were taken and compared to the values of pure diesel. The following Table 1 displays the specification of VCR engine.

Table 1. Engine specifications

Engine	Make Kirloskar, 1 Cylinder, 4 Stroke, Water cooled
Stroke and Bore	110 mm X 87.5 mm
Rated Power	3.5 kW at 1500 rpm
Load at Rated Power	12kg
Compression Ratio Range	14-18
Stroke Volume	661cc
Dynamometer	Eddy Current Dynamometer

3 Results and Discussion

3.1 Comparison between all the Blends considering VCR 17.5

Brake Power versus Load. Fig. 2 shows brake power vs. load for various blends at VCR 17.5.

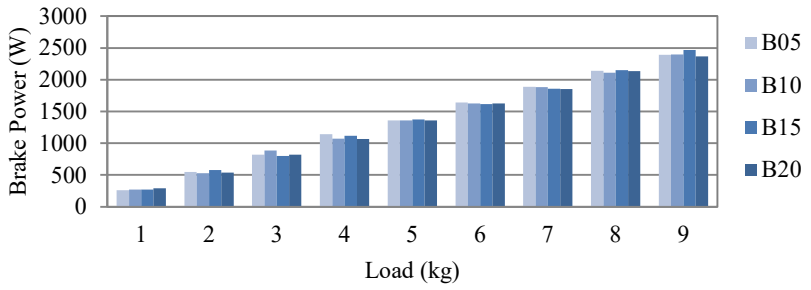

Fig. 2. Brake power versus load for various blends at VCR 17.5

A gradual linear growth in brake power can be observed as engine load increases. As the load increases the torque increases and torque is directly dependent on brake power. Considering the readings from the report generated by the engine, it can be observed that for blends B15 and B20, brake power generated is approximately better at some loads.

Brake Specific Fuel Consumption versus Load. It is observed that, there is a gradual decrease in the value of brake specific fuel consumption (BSFC) as the load increase. The reason for this behavior is that as the load increases torque increases which leads to an increase in brake power and it is known that BSFC is inversely proportional to brake power. This trend is also observed due to lower heating value and higher viscosity of biodiesel. As understood from the Fig. 3 at 1 kg load the BSFC of B20 blend is the least. At higher loads, the comparatively lower BSFC of B20 is maintained.

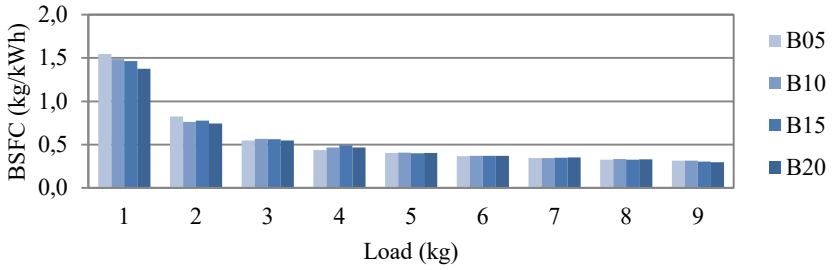

Fig. 3. Brake specific fuel consumption versus load for various blends at VCR 17.5

Mechanical Efficiency versus Load. Fig. 4 shows mechanical efficiency vs. load for various blends at VCR 17.5. It is observed that, mechanical efficiency gradually increases with an increase in load, the reason for this trend is that mechanical efficiency is directly proportional to brake power so as the load increases brake power increases and leads to an increase in mechanical efficiency.

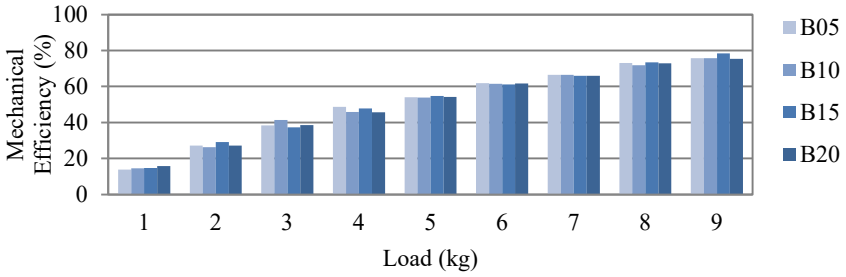

Fig. 4. Mechanical efficiency versus load for various blends at VCR 17.5

Looking at the data found in the readings and the graph, it can be observed, that the mechanical efficiency performs slightly better for B20 in most load conditions.

Brake Thermal Efficiency versus Load. Fig. 5 shows brake thermal fuel efficiency (BThE) versus load for various blends at VCR 17.5. It can be observed, that the BThE increases with an increase in load. This is because, at higher loads, the turbulence and

the temperature inside the combustion chamber i.e. the cylinder will be high which helps in the atomization and proper mixing of fuel resulting in higher efficiency. Looking at the data plotted in Fig 5, it is understood that for VCR 17.5 B20 gives the optimum brake thermal efficiency.

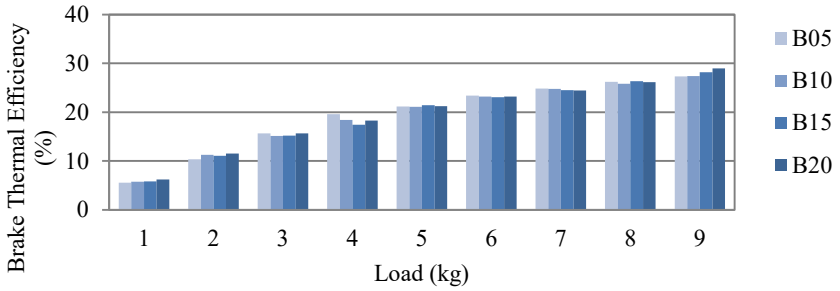

Fig. 5. Brake thermal efficiency versus load for various blends at VCR 17.5

Thus from all the graphs and readings at VCR 17.5, it can be concluded that the B20 biodiesel blended fuel is giving favorable or improved performance when performance analysis is considered and it also provides the optimum results for all the parameters.

3.2 Comparison of B20 Blend with Pure Diesel at VCR 17.5

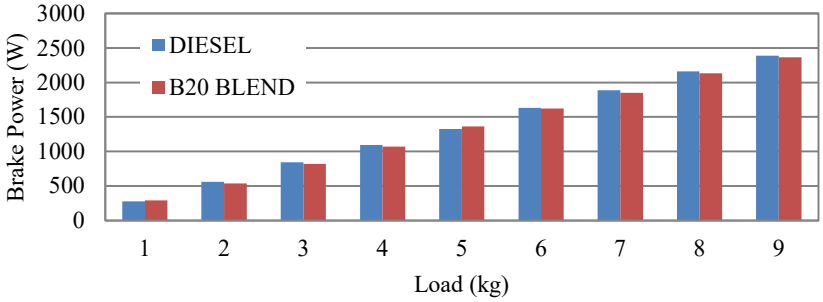

Fig. 6. Brake power versus loads for diesel and B20 at VCR 17.5

Brake Power versus Load. Fig. 6 shows brake power versus load for the B20 blend and pure diesel. It can be observed, that brake power for B20 is almost similar to that of diesel at each and every load. That means, as far as brake power is concerned, B20 performs in the same manner as pure diesel at every load.

Brake Specific Fuel Consumption versus Load. Fig. 7 shows brake specific fuel consumption (BSFC) versus load for the B20 blend and pure diesel. It can be observed, that BSFC is minimum or identical for B20 compared to pure diesel at a maximum number of loads. Thus as per BSFC also, B20 performs in an equivalent manner as pure diesel at every load.

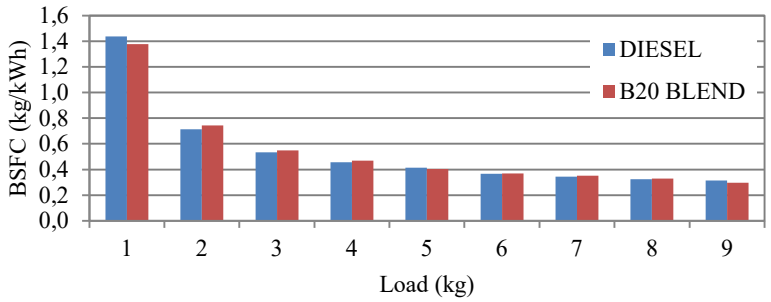

Fig. 7. Brake specific fuel consumption versus load for diesel and B20 at VCR 17.5

Mechanical Efficiency versus Load. Fig. 8 shows mechanical efficiency versus load for the B20 blend and pure diesel. It can be observed, that for the maximum amount of loads, the mechanical efficiency performs better or is equivalent for B20 compared to that of pure diesel. Thus for mechanical efficiency also it can concluded that B20 is better fuel.

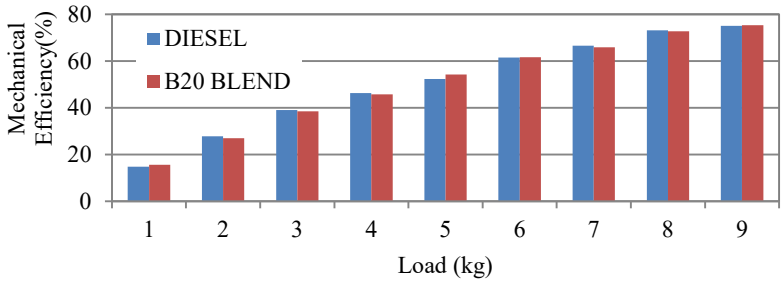

Fig. 8. Mechanical efficiency versus load for diesel and B20 at VCR 17.5

Brake Thermal Efficiency versus Load. For brake thermal efficiency also it can be observed, that for maximum amount of loads, BThE performs identical for B20 and diesel. For load 1kg, the BThE value observed for diesel is 5.26 and for B20 is 6.23. Similarly at 9kg value for diesel is 27.28 and for B20 is 28.96. Therefore as far as performance analysis is concerned, B20 can be considered as an alternative fuel option for the current situation.

Regression analysis (Minitab) showed that the compression ratio of 17.5 and the blend B20 gave the most optimum results. The confidence values of brake power and brake thermal efficiency were at 90% and 93% respectively. The error may have occurred due to the weak foundation, excessive vibrations, more heat loss and more. Other values such as torque, mechanical efficiency, and brake specific fuel consumption are above 95% confidence levels. Therefore, the results can be relied on the experiment.

4 Conclusion

Firstly, it was found that at optimum compression ratio 17.5, the performance analysis using all blends of biodiesel, B20 had good performance values compared to other biodiesel blends. A detailed analysis was carried out using pure diesel and B20 biodiesel blend, in which it was concluded that B20 had higher or identical brake power, lower brake specific fuel consumption, and higher mechanical efficiency at maximum numbers of loads. Thus, while carrying out the performance analysis on the variable compression ratio engine at VCR 17.5 using diesel and biodiesel blends, it was found that the optimum values for performance were at generated for B20 biodiesel blend when compared to pure diesel. So, experimentally it was observed that without changing the configuration of present diesel engines a biodiesel blend up to 20% of biofuel can be used as a good alternative for pure diesel.

References

1. V. Rambabu, Dr.V.J.J.Prasad, Dr.T.Subramanyam, D., “Evaluation of Performance and Emissions of a VCR DI Diesel Engine Fuelled with Preheated CsME," Global Journal of Research In Engineering, vol. 12, 2013. [Online]. Available: https://www.engineeringresearch.org/index.php/GJRE/article/view/687. [Accessed: 27 May 2019].
2. K. Muralidharan, D. Vasudevan and K. N. Sheeba, "Performance, emission and combustion characteristics of biodiesel fuelled variable compression ratio engine," Energy, vol. 36, pp. 5385-5393, 8 2011. Retrieved from https://doi.org/10.1016/j.energy.2011.06.050
3. D.N.Mallikappa, R. Pratap Reddy and Ch. S N Murthy, "Performance and Emission Characteristics Studies on Stationary Diesel Engines Operated with Cardanol Biofuel Blends," International Journal of Renewable Energy Research, vol. 2, 1 2012.
4. G. Pavan, M. Rajesh and K. Srinivas, "Performance and Exhaust Emissions Using Blends on VCR Diesel Engine with Varying Compression Ratio of Hibiscus Oil," International Journal of Engineering Trends and Technology, vol. 17, pp. 94-102, 11 2014.
5. K. I. Yapici, "Compression ratio setting device for an internal-combustion engine". United States of America Patent US6247430B1, 30 10 1998.

6. "Combustion and Emission Characteristics of Variable Compression Ignition Engine Fueled with Jatropha curcas Ethyl Ester Blends at Different Compression Ratio - Scientific Figure on ResearchGate.," [Online]. Available: https://www.researchgate.net/figure/Schematic-diagram-of-the-experimental-setup_fig1_275063782. [Accessed: 26 May 2019].

Analysis and Evaluation of the eHighway System on the Basis of Technical, Ecological and Economic Criteria

- a comparison of three types of drives -

Vincent Rudolph[1] and Kathrin Hesse[2]

[1] M.Sc. student, Düsseldorf University of Applied Sciences, Germany
vincent.rudolph@study.hs-duesseldorf.de

[2]Cologne University of Applied Sciences, Cologne, Germany

Abstract. Forecasts show that road transport volumes will increase strongly in the coming years. Here the greatest challenge lies in decoupling the growing volume of transport and the resulting emissions from each other. In this paper, which is based on data available in 2017, the potential of an electric hybrid truck system, powered via overhead power lines, called "eHighway", is analyzed and compared to electric and diesel trucks. For the comparison, a future scenario and a scenario that is conceivable today have been set up. The results show that the "eHighway" system represents an already available solution for reducing CO_2 emissions from road freight transport, that could contribute to achieving the climate goals. It also shows how dependent an ecologically and economically sensible electrification of freight transport is on the share of renewable energies in the German electricity mix.

Keywords: eHighway, road freight transport, greenhouse gas emissions, energy consumption, drive types.

1 Introduction

The entire German freight traffic in transport logistics has grown steadily in recent years [1]. The 'modal split', as the distribution of the transport volume among the various types of transport is called [2], shows that road freight transport accounts for the largest share of transport services. The problem caused by the high volume of traffic on German roads lies not only in coping with the increased transport services, but increasingly in consuming finite resources and polluting the environment. Although this applies to all modes of transport, road transport is by far the most polluting mode of transport for freight, accounting for around 81% compared with the other modes of transport: rail and inland waterways [3]. Despite continuous technical improvements, absolute CO_2 emissions from road freight transport increased by 11% between 1995 and 2010 due to the growing traffic volumes [2]. In the past, the demanding environmental standards of the European emission norms (EURO norm) have constantly promoted the development of technical solutions for the reduction of pollutant emissions

and continue to do so today. According to the 2030 traffic network forecast of the Federal Ministry of Transport and Digital Infrastructure (BMVI), transport volumes and road transport performance will continue to increase continuously in the future. The volume of goods transported on the road will rise to 72.5% by 2030 [3]. Against this background, the call for companies to find sustainable logistics solutions is increasing. Regardless of the enormous progress made in recent years in the areas of pollutant reduction and fuel saving, the greatest challenge lies in decoupling the growing volume of transport and the resulting emissions from each other. In view of the high proportion of environmentally harmful emissions in road freight transport, trucks and in particular their drive systems are the focus of research. At present, however, the share of diesel engines in the total truck fleet in Germany is still 95% and therefore represents the standard drive type for trucks. This clearly shows that alternative solutions, such as electric or hybrid trucks, are not yet established in road freight transport. To achieve the national climate targets, which require a 70% reduction in greenhouse gas (GHG) emissions between 1990 and 2040, alternative drive systems will be needed in the future [4].

2 The eHighway System

The eHighway system is a new approach to reduce emissions like greenhouse gases, noise and exhaust gases in road freight transport. Trucks driving with the eHighway system have a conventional diesel combustion engine, but can also be powered purely electrically, therefore this system is a parallel hybrid. The unique feature of this system is, that the electric motor of the truck is not powered by a battery. The required energy is provided by an overhead contact line to which the truck is connected via a current collector, that enables a continuous power supply to the vehicle (see Fig.1). Here the old technology of trolleybuses and the concept of current collectors of resource-saving electric railways was combined with the flexibility of road freight transport. To establish a connection with the power line, a scanner checks at any time whether there is an overhead line above the vehicle. If an overhead line is detected, the current collector, also known as pantograph, either connects automatically to the overhead line or is triggered by the driver at the push of a button. In order to maintain constant connection to the overhead contact line, the pantograph aligns itself continuously under the overhead contact line and compensates slight position deviations within the lane.

Fig. 1. Electrified Scania G360 4x2 on an eHighway test track [6].

This technology, which was patented by Siemens [5], prevents punctual wear of the pantograph and preserves the driver's familiar operating procedures. During overtaking maneuvers or when driving on unequipped roads, the pantograph retracts and the combustion engine restarts without any power reduction during the mode change. Attaching and detaching of the pantograph can be performed at speeds from 0 to 90 km/h smoothly and without any risk. During the electric driving, the small battery of the truck can be charged with electricity from the power line and with the energy generated by breaking, known as recuperation, where kinetic energy is converted back to electric energy. If this recuperation produces excess energy, it can be made available to other vehicles in the system or fed back into the higher-level power grid [7]. The eHighway system also has the advantage that existing roads can be equipped with the eHighway infrastructure and remain fully usable for other road users [8].

3 Comparison of Drive Types

To evaluate the potential of the eHighway system, the diesel-electric hybrid drive system was compared with two other drive concepts used in road freight transport. These include the conventional diesel drive and the purely battery electric drive. To make the drive systems comparable, a practical example of a truck model with comparable technical data was used for each drive type. All three models have a total towing weight of 40 tons, a wheelbase of 3.7/3.8m and from 360 to 475 horsepower.

3.1 Methods

The European standard EN 16258 " Methodology for calculation and declaration of energy consumption and greenhouse gas emissions in transport services" was used to compare the drive types using the criteria energy consumption and greenhouse gas emissions [9]. This standard is well suited for this purpose, as both Tank-to-Wheel (TTW) and Well-to-Wheel (WTW) emissions and consumption are considered in the calculation. For TTW and WTW, the measured energy consumption is multiplied by the specific conversion factor [10]. However, these conversion factors had to be adapted before the actual calculation. This was necessary because the standard values refer to 2013 and since then the share of renewable energies has increased in the German electricity mix (status as of 2016) [4]. With these electricity mix specific energy and emission factors the absolute energy consumption and greenhouse gas emissions can be calculated.

For an economic comparison of the trucks, the costs for one year and a mileage of 100,000 km were calculated for each drive type. The annual costs include tolls, taxes and energy/fuel costs.

A qualitative comparison was also carried out to evaluate the three drive types regarding twelve different criteria. The criteria range, refueling time, energy consumption, efficiency, GHG-emission TTW, GHG-emission Well-to-Tank (WTT), air pollutant emission, infrastructure expansion, adjustment expenditure/acquisition costs, road tolls, taxes and energy costs, have been determined. In order to highlight the advantages

and disadvantages of the drive concepts, each criterion is assessed per practical example with a double plus (++), a plus (+), a circle (o), a minus (-) or a double minus (- -), depending on whether the criterion indicates that the drive concept is in favor of or against the concept, as shown in Table 1.

Table 1. Assessed criterions per practical example

criterions	electric drive	hybrid drive (eHighway)	diesel drive
range	- -	o	++
refueling time	- -	++	++
energy consumption	+	+	o
efficiency	+	++	-
GHG-emission TTW	++	o	- -
GHG-emission WTT	-	o	+
air pollutant emission	++	+	- -
infrastructure expansion	++	- -	++
adjustment expenditure/ acquisition costs	--	-	++
road toll	+	+	-
taxes	+	o	-
energy cost	-	++	+

3.2 Two Scenarios

Two different scenarios were defined for the calculation. In the first scenario, the values for fuel and energy consumption, the composition of the German electricity mix, and the electricity and diesel prices refer to data from 2016.

The second scenario is a conceivable future scenario. It is assumed that 65% of the electricity generated will come from renewable energies and all electricity from nuclear power, lignite and hard coal will be omitted. In addition, it is assumed that the efficiency of diesel trucks will steadily increase, thus reducing fuel consumption. The efficiency of the eHighway trucks and electric trucks has also been adjusted to prognoses. Here an energy consumption of 160 instead of 180 kWh/100km is expected [11]. It was also expected that the price of diesel, which includes a CO_2 tax, would rise [12]. For the eHighway system it can be assumed that the price per kWh will increase by 20%, as it is a government-sponsored project and for the electric truck by 40% [13]. The different prices arise because the electricity price is calculated according to the company's annual consumption.

Furthermore, in the second scenario it is expected that there will be no taxes or charges for driving an electrically powered truck. For the hybrid truck, it can be assumed that the toll is waived for every kilometer driven with electricity. In order to be able to compare the scenarios despite the changed parameters, the following framework conditions were defined for both scenarios:

- Fully loaded semitrailer truck (40t)
- Highway ride
- Annual mileage: 100,000 km
- 50% electrified overhead line section
- Tolls on 80% of the route
- Limited range of the electric truck & charging stops not taken into account.

4 Results

4.1 Energy Consumption

The results show that all values (TTW and WTW) in scenario 2 are well below those in scenario 1 (see Fig. 2). On the one hand, this is due to the lower direct fuel and energy consumption, but on the other hand it is primarily due to the increase in renewable energies. A comparison of indirect energy consumption clearly shows the significant influence of the increase in renewable energies in the German electricity mix on the overall energy supply and therefore on the efficiency of the vehicles.

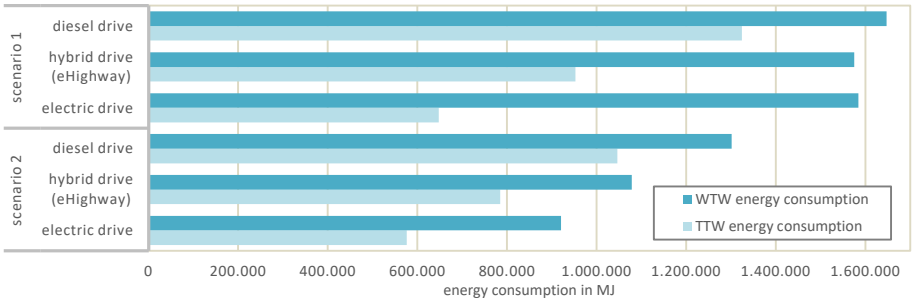

Fig. 2. Results of the annual direct (Tank to Wheel) and overall (Well to Wheel) energy consumption of the different drive types in scenario 1 (data from 2016) and scenario 2 (conceivable future scenario)

4.2 Greenhouse Gas (GHG) Emissions

The increase in renewable energies in the electricity mix to 65% and the improvement in energy consumption lead to a reduction in GHG emissions of around 80% for electric truck. At present, the electric truck is not very environmentally friendly despite emission-free driving, as it only produces 20% less GHG in total than a conventional diesel truck. The diagram also shows that, under current conditions, implementing the eHighway system could save around 40 tons of CO2 equivalents (CO2e) compared to diesel. The results are shown in the diagram in Figure 3.

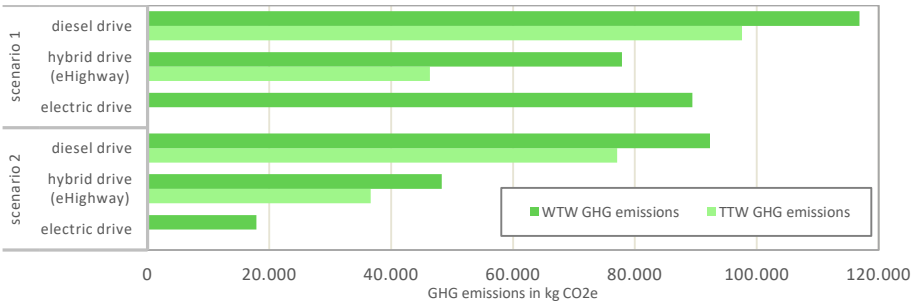

Fig. 3. Results of the annual direct (Tank to Wheel) and overall (Well to Wheel) GHG emissions of the different drive types in scenario 1 (data from 2016) and scenario 2 (conceivable future scenario)

4.3 Cost Calculation

Figure 4 shows the annual cost per drive type in both scenarios, including energy/fuel cost, taxes and road toll. A comparison of the diesel and the eHighway truck shows that the eHighway system can already offer an advantage over diesel under today's conditions. A haulage company operating an eHighway truck could save around 27% a year, or around €14,000. According to Nils-Gunnar Vågstedt, Chief Engineer at Scania, the cost of converting a conventional truck to a trolley truck will be around €10,000 to €40,000 [14]. With annual cost savings of around €14,000, the conversion costs could be covered after just one to three years. The considerable increase in costs for the use of diesel trucks makes it clear that, especially in the future, when diesel prices rise, a changeover to alternative drive systems will not only protect the environment, but also be economically viable.

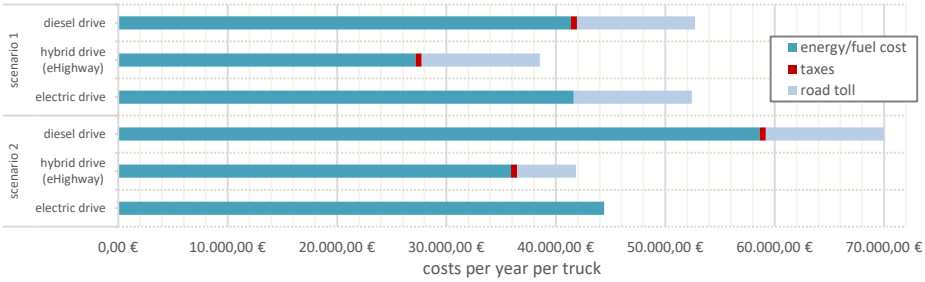

Fig. 4. Annual costs of the different drive types in scenario 1 (data from 2016) and scenario 2 (conceivable future scenario)

4.4 Qualitative Comparison

To illustrate the results of the qualitative comparison, a web diagram was created to show the score of each practical example, as shown in Figure 5. The further the data points are at the edge of the diagram, the better the result.

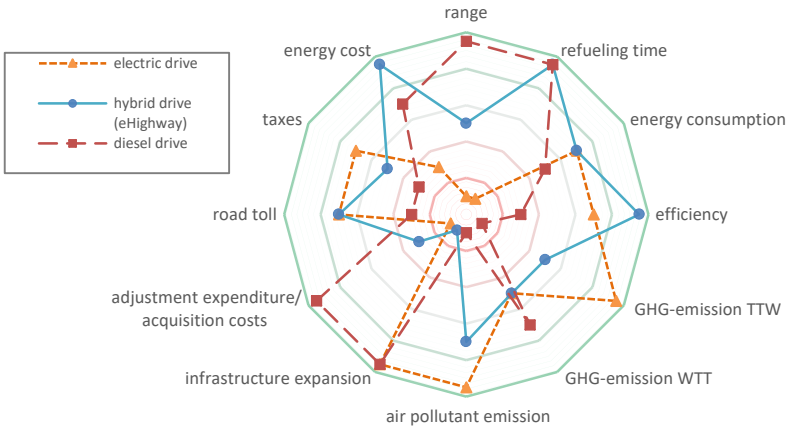

Fig. 5. Results of the qualitative comparison displayed in one web diagram. The further the data points are at the edge of the diagram, the better the result.

5 Conclusion

It has been shown that the conventional diesel truck is optimally suited for long-distance transport, but in view of the stricter environmental criteria and a future increase in fuel prices, the diesel truck will lose its ecological and economic advantage in the future.
It has also become clear that battery-powered trucks have a great potential for freight transport, but with the technologies available today, they are not yet suitable for long-distance freight transport [15].

Apart from the high investment costs, the potential of the innovative eHighway system has been demonstrated. The electrification of the motorway therefore represents a possible solution for reducing CO_2 emissions in road freight transport, which could contribute to meeting the climate targets. A decisive advantage is that the technology required to implement the eHighway system is already available today, compared to trucks purely powered electrically. It is also made clear, that in order to achieve the climate targets, the electricity mix in Germany must continue to change in favor of renewable energies. Only then, the electrification of freight transport will become ecologically and economically beneficial.

In summary, it can be said that only when emission regulations are further tightened, diesel prices continue to rise, the share of renewable energies in the German electricity mix increases and either battery technology makes significant progress or an overhead line infrastructure exists, actual change in long-distance freight transport is conceivable.

References

1. Mehlin, M.; Zimmer, W.: Ein Weg für klimagerechte Mobilität? *INTERNATIONALES VERKEHRSWESEN* 62(5), 10-15 (2010).
2. Wittenbrink, P.: Green logistics. Konzept, aktuelle Entwicklungen und Handlungsfelder zur Emissionsreduktion im Transportbereich, Springer Babler, Wiesbaden (2015).
3. Schubert, M.: Verkehrsverflechtungsprognose 2030, Bundesministerium für Verkehr und Infrastruktur, Berlin (2014).
4. Shell Deutschland und DLR: Shell Nutzfahrzeug-Studie 2016. Diesel oder alternative Antriebe - Womit fahren LKW und Busse morgen?, Shell Deutschland (2016).
5. Engdahl, H., Francke, J., Gerstenberg, F., Graebner, O., Lehmann, M., Goeran S., Buehs, F.: Vehicle control system and method for automated driving of a specific lane for continuous supply with electrical energy. USA Patent 10108201, October 23 2018.
6. Spiegel Online: Modellversuch Elektro-Autobahn Gehört dem Oberleitungs-Lkw die Zukunft?,
7. https://www.spiegel.de/plus/e-highway-gehoert-dem-oberleitungs-lkw-die-zukunft-a-00000000-0002-0001-0000-000165579694. last accessed 2019/11/06.
8. Sachse, T., Grabner, O., Mockel, M., Kaschwich, C., & Plattner, J. : Intelligent traffic control and optimization with cooperative systems on the eHighway: Using the electrified highway-infrastructure for heavy good vehicles and the advanced traffic control center with V2X for a more efficient and safer traffic (for all road users), International Conference on Connected Vehicles and Expo (ICCVE), Vienna, 2014, pp. 558-560.
9. Siemens: eHighway – Electrification of road freight transport, https://new.siemens.com/global/en/products/mobility/road-solutions/electromobility/ehighway.html. last accessed 2019/05/10.
10. DIN EN 16258:2013-03, Methodology for calculation and declaration of energy consump-tion and GHG emissions of transport services (freight and passen-gers); German version EN (EN 16258:2012)
11. Schmied M., Mottschall, M., Berechnung des Energieverbrauchs und der Treibhausgasemissionen des ÖPNV. Leitfaden zur Anwendung der europäischen Norm EN 16258, Bundesministerium für Verkehr und digitale Infrastruktur, Berlin (2014).
12. Fraunhofer ISI, Machbarkeitsstudie zur Ermittlung der Potentiale des Hybrid-Oberleitungs-Lkw, Bundesministerium für Verkehr und digitale Infrastruktur, Berlin (2017).
13. Hammar, H., Jagers, C.: What is a fair CO_2 tax increase? On fair emission reductions in the transport sector, *ECOLOGICAL ECONOMICS* 61(2-3), 377 – 387 (2007).
14. Schlesinger, M., Lindenberger, D.: Entwicklung der Energiemärkte-Energiereferenzprognose, Osnabrück, (2014).
15. Vågstedt, N.-G.: *E-Mail (written in English), (*2017)
16. Cano, Z., Banham, D., Ye, S. Hintennach, A., Lu, Y., Fowler, M.: Batteries and fuel cells for emerging electric vehicle markets, *Nature Energy* 3(4), 279–289 (2018).

Fabrication and Analysis of Human Hair Based Hybrid Epoxy Composite for Mechanical Properties and Applications

Venugopal Vatsal[1] and Shaik Shamveel[2]

[1] M.Sc. student, Düsseldorf University of Applied Sciences, Germany
vatsal.venugopal@study.hs-duesseldorf.de

[2] Dr.M.G.R University,Chennai, India

Abstract. Tensile, flexural, impact strengths, hardness and inter laminar distribution of human hair based hybrid epoxy composite were evaluated to assess the possibility of using it as a new material in engineering applications such as automobile and aircraft applications for longevity. Addition of epoxy to the human hair fiber ensures strength. Samples were fabricated by the hand lay-up process (37.5:62.5 fiber to matrix ratio by weight) and the mechanical properties like tensile, flexural and compressive strength were evaluated using a universal testing machine. Hardness test was conducted using Rockwell hardness testing machine, Impact test using Izod impact test method and Inter De-laminar test using three-point loading followed by observation under HD camera. The primary focus, however, were the Tensile and Flexural strengths for the human hair based hybrid epoxy composite laminates which were calculated to be 36.9 MPa and 7.86 MPa respectively. The fabricated material's properties were then used to check the mechanical strength by means of a Drop test simulation using SolidWorks by Dassault Systems for an application in the form of a bumper to illustrate the comparative strength of this material compared to poly-carbonates currently in use. The investigated hybrid epoxy turned out to be sustainable and cost effective solution for various applications.

Keywords: human hair, epoxy, tensile strength, flexural strength, hardness, impact strength, inter de-lamination.

1 Introduction

A composite material may be defined as a combination of two or more materials that leads to better properties than those of the individual components used alone [1]. In comparison with metallic alloys, each material retains its separate chemical, physical and mechanical properties. The two main constituents are a fiber and a matrix. The main merits of composite materials are their high stiffness and strength, combined with low density when compared with bulk materials, allowing a weight reduction of the finished material. The reinforcing phase provides the strength and stiffness. In most cases, the reinforcement is harder, stronger, and stiffer than the matrix. A fiber has a

length that is much greater than its diameter. The length-to-diameter (l/d) ratio is known as the aspect ratio and can vary vastly. Continuous fibers have long aspect ratios, while discontinuous fibers have shorter aspect ratios. Continuous-fiber composites normally have a regular orientation, while discontinuous fibers generally have a random orientation.

1.1 Human Hair – Theoretical Introduction

Hair threads form a major part of the external covering of most mammals. The hair thread has a cylindrical structure, highly organized, and formed by inert cells. Hair forms a very rigid structure in the molecular level, which is able to offer the thread both flexibility and mechanical resistance [2].

Human hair contains about 65-95% of its weight in proteins, more 32% of water, lipid pigments and other components. Chemically, about 80% of human hair is formed by a protein known as keratin [3].Threads present significant structural differences across ethnic groups and within the same group. The factors important are: resistance, elasticity, diameter, bending and shape of the cross section. One may handle it and apply products to mimic differences of the touch sensorial characteristics; these are, however, transient effects [4].

The unique properties of human hair, such as its chemical composition, slow degradation rate, high tensile strength, thermal insulation, elastic recovery, scaly surface and unique interactions with water and oils, along with its socio-cultural roles, have led to many diverse uses. These uses also depend on the variety of hair available, varying in terms of five parameters: length, color, straightness or curliness, hair damage, and contamination [5].

1.2 Preliminary Tests on Human Hair

Tensile test was conducted on hair strands in an attempt to determine the strength of individual follicle of hair. It was observed that the resulting strength was between 320 and 350 MPa.

On the contrary, the previous works involved the development of similar materials using animal hair, for example, goat hair which has a tensile strength of 90 to 120 MPa [6].

Density of the human hair was determined by using Archimedes' principle and was found out to be 1150 kg/m^3 which meant that it could be helpful in making the composite material lighter.

2 Fabrication

2.1 Preparation

The composite was made by collecting hair from various sources and making them into beds of minute thickness in such a way that the follicles are interlocked. Taking approximately 0.02 kg of hair for each bed, three such beds were made. A bunch of approximately 100mm long hair was taken and small groups of follicles were formed each of approximately the same thickness and placed separately longitudinally. The epoxy resin comprised of Araldite LY556 to HY951 hardener in the ratio of (10:1) [7].

Fig. 1. Bunches of Hair follicles

2.2 Fabrication Process

Epoxy resin is the most widely used material due to its prevalent mechanical and thermal properties even at elevated temperatures. It also exhibits low shrinkage after curing and great synthetic safety. LY556 Epoxy and HY951 hardener are used as matrix material with a mixing ratio of 10:1 by weight [7]. An epoxy matrix of 62.5% by weight is used.

A portion of the mixed resin was applied on the inner side of the template. Then one of the rolled bed of hair was placed and arranged precisely within the boundaries. This was allowed to dry for some time, before the second layer of epoxy was poured on top of it and spread evenly by using a mild steel roller held by a handle. Then the single hair strands, about 25, were placed longitudinally, uni-directionally on top of the resin. Then the epoxy resin was poured on top of the second bed and evenly spread. The same procedure was followed for two more layers. Then the remaining strands were placed on the top as the last layer with an orientation at 0° with reference to previous layer of strands and all the remaining epoxy was poured on top. Then 4 mm thick spacers were placed at the vertices of the template in order to ensure non-tapered surface and even thickness throughout. The entire set-up is laid between two parallel mold plates and weights are added in order to compress and compact the material which is left undisturbed for about 48 hours to cure. The compression molded composite was left undisturbed for one day. After the composite was fabricated it was cut into 200*200mm dimensions and the weight was measured as 200gms (125gms. of Epoxy resin and 75gms. of hair fiber).

Fig. 2. Fabricated material cut into various shapes and dimensions for testing according to ASTM standards

3 Testing and Results

The primary focus of performing these undermentioned tests is to check the strength and durability of the material that was fabricated.
The strength tests work on the formula of stress, i.e.

$$Stress = Load \div Area \tag{1}$$

3.1 Tensile Test according to ASTM D638-03

Tension testing is a fundamental materials science test in which a specimen is subjected to a controlled tension until failure [9].The specimen was loaded in a servo-assisted hydraulic universal testing machine (UTM) with a gauge length of 120 mm. The speed of testing was set at a rate of 1 mm/min and the machine was started. As the specimen elongates, the resistance of the specimen increases, which is measured by a load cell to obtain a stress-strain curve.

Fig. 3. Specimen for tensile test in UTM

The experimental values of tensile stress vs strain for composite specimens were plotted and have been shown in Fig 4. The obtained tensile strength was 36.9 MPa at 2.2% strain and the Young's Modulus was 3 GPa.

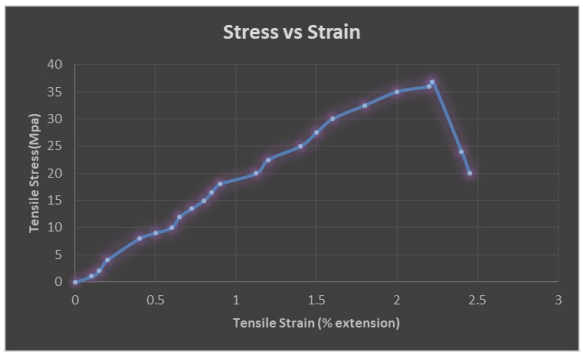

Fig. 4. Stress-strain curve of human hair epoxy composite

3.2 Flexural Test according to ASTM D790

The flexural properties of the composites were evaluated using the UTM with a cross head speed of 1 mm/min and a span length of 50 mm. The flexural strength was measured as per the ASTM D 790 standard [9]. Three-point loading was applied. The deflection of the specimen was continued until a rupture of the specimen was observed at a maximum flexural strength value of 7.86 MPa at approximately 3.7% strain.

3.3 Impact Test according to ASTM D256

The ASTM International standard for Izod Impact testing of plastics is ASTM D256 [10].Impact testing is done for determining the toughness of a material against sudden force or impact. Izod impact testing is an ASTM standard method of determining the impact resistance of materials. A pivoting arm is raised to a specific height (constant potential energy) and then released. The arm swings down hitting the sample and breaking the specimen. The energy absorbed by the sample is calculated from the height the arm swings to the point when hitting the sample. A notched sample is generally used to determine impact energy and notch sensitivity.

It was seen that the impact strength value was 6 Joules for the composite.

3.4 Inter De-laminar Test according to ASTM D2344 [11]

Inter de-lamination is the property of a material to show its bending capacity whilst displaying its internal distribution of fibre and resin, in case of polymer. Three-point loading was applied on this beam until the material fractured. The total fracture is then viewed under a high-definition camera for the inter de-lamination images.

The images showed that epoxy distribution is uniform, compaction is good, fibres are distributed evenly, bonding of hair with epoxy is good, material behaviour is normal. The bonding can be determined from the fact that the bending stress was about 7.86MPa which is quite good for fibre composites.

Fig. 5. Inter de-laminar test image of human hair epoxy composite

3.5 Hardness Test according to ASTM D785

The hardness testing of plastics is most often measured by the Rockwell hardness test [12]. It measures the resistance of the plastic towards indentation, providing an empirical hardness value. Rockwell hardness is generally chosen for 'harder' plastics such as polycarbonate or polystyrene, where the resiliency or creep is less likely to affect the results.

Rockwell hardness test were carried out and hardness at four different locations were measured. The average value of hardness obtained was. 36.33 RHN.

Table 1. Summary of Mechanical test results

Test Type	Result
Tensile Strength	36.9 MPa
Flexural Strength	7.86 MPa
Impact Strength	6 J
Hardness	36.33 RHN

4 Applications

This composite fabrication was aimed at producing durable bumpers as a primary application using hair fibre with epoxy resin.

Software models (SolidWorks 2015 by Dassault Systems) [13] of various profiles were generated, with the properties of the fabricated material and normal poly-carbonate material available in order to draw comparisons between the stress bearing capacities.

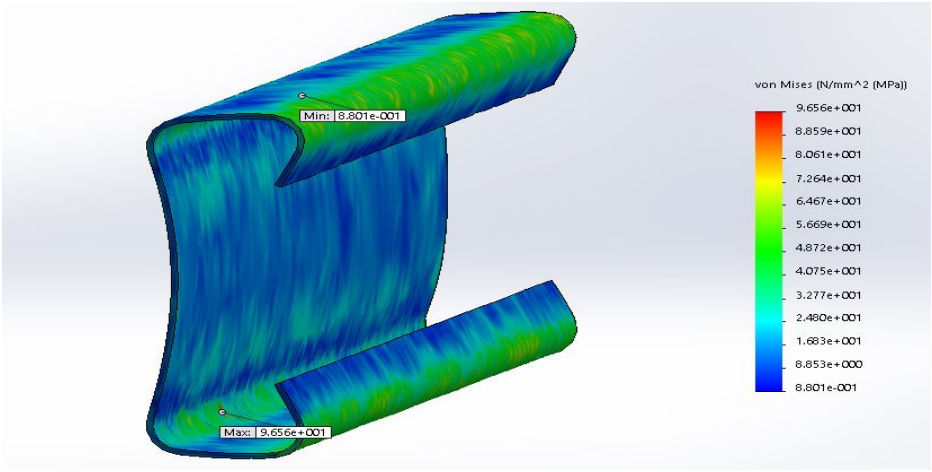

Fig. 6. Simulation model of a bumper (channel section) made of hair composite material and its stress characteristics using Drop test

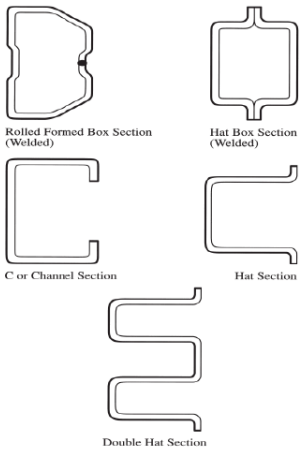

Fig. 7. Different profiles of bumper

Table 2. Maximum stress values obtained in drop test simulation for different materials for different bumper profiles in N/mm^2 (MPa)

Profile	Polycarbonate material	Human Hair Composite material
Channel	78.2	96.56
Double Hat	37.12	58.56
Hat	38.93	50.27
Hat Box	77.73	124.8
Rolled Formed Box	99.07	128.3

Further, the applications over this material can be extended in other automobile and aircraft applications, where there is a need for vibration and noise damping. It is also a good water-proof and fire proof material due to the addition of epoxy. Practical possible applications of this materials include car bumpers, aircraft noses, engine covers, fuel tanks etc.

5 Conclusions

The tensile strength value of hair fibre epoxy composite is very good for plastics and is in line with other similar experiments with composite materials [8] [14]. The flexural strength of the composite is also remarkable [8]. The enhanced flexural properties are due to the formation of a thick bonding network structure between the hair strands and the epoxy matrix.

The tensile strength value is close to 37 MPa in the fabricated material which is from human hair. In comparison to this a few previous works with animal hair (goat hair) resulted in material having strength of 33.9 MPa [15] and a slight increase to 36 MPa when adding additives like graphene [6]. Although not a significant increase it still can be considered that the use of human hair over animal hair was a good choice to improve mechanical properties.

The impact strength and hardness number in Rockwell scale C indicate that the material is considerably tough and moderately hard. Also, the inter de-lamination images suggest that resin distribution is uniform, compaction is good, fibres are distributed evenly.

Additionally, the density of the fabricated material is calculated to be around 1250 kg/m^3 which is not so different from a polycarbonate material which has a density of 1200 to 1225 kg/m^3.

Furthermore, the comparative values of the stress levels of the different bumpers clearly show that the fabricated material has superior properties compared to the locally available poly- carbonate and hence can be used as an efficient alternative.

Hence, it can be concluded that the hair fibre epoxy composite shows better strength compared to a regular polycarbonate when tested for the same purpose(as a bumper in this case). However, these results may vary depending on the type of fabrication, fibre to matrix ratio and the number of layers of the individual constituents. It has a good

scope of development, a wide spread usage and also good combining abilities. It is an eco-friendly, long life and cost effective solution for various applications.

References

1. Wikipedia, https://en.wikipedia.org/wiki/Composite_material#Composite_materials, last accessed 2018/12/11.
2. Longo, V.M.; Monteiro, V.F.; Pinheiro, A.S.; Terci, D.; Vasconcelos, J.S.; Paskocimas, C.A.; Leite, E.R.; Longo, E.; Varela, J.A. Charge density alterations in human hair fibers: an investigation using electrostatic force microscopy. *Int. J. Cosmet. Sci.*, Oxford, v.28, n.2, p.95-101, (2006).
3. Wagner, R.C.C.; Joekes, I. Hair protein removal by sodium dodecyl sulfate. Colloids Surf. B Biointerfaces, Amsterdam, v.41, n.1, p.7-14, (2007).
4. Juez, J.L.; Gimier, L. Ciencia cosmética. 2.ed. Madrid: Soc. Espanhola de Quim. Cosmet., p.98-119 , (1983).
5. Ankush Gupta, Human hair "waste" and its utilization: Gaps and Possibilities, Journal of Waste Management, Volume 2014, Article ID 498018, Hindawi Publishing Corporation, (2014).
6. The effect of fibre loading and graphene on the mechanical properties of goat hair fibre epoxy composite J Jayaseelan*, K R Vijayakumar, N Ethiraj, T Sivabalan and W Andrew nallayan Mechanical Engineering Department, Dr M.G.R Educational and Research Institute University, Maduravoyal, Chennai-600095, India.
7. Ronald Charles Allum, Philip Michael Durbin, Patent No. US 9267018 B2, (Publication Date:02/23/2016)
8. J. Jayaseelan, P. Palanisamy, K.R. Vijayakumar and A. Dhanam Maria Vinita, Int. J. Vehicle Structures & Systems, 7(4), 165-168, . MechAero Foundation for Technical Research & Education Excellence, (2015)
9. American Society for Testing and Materials (ASTM), 2000.ASTM D 638-99-2000 and 790-99-2000. ASTMCommittee on Standards. West Conshocken, PA, pp. 1-13 and 145-151, (2000).
10. Wikipedia Homepage for Izod impact test, https://en.wikipedia.org/wiki/Izod_impact_strength_test, last accessed 2019/12/26
11. ASTM International Homepage, https://www.astm.org/Standards/D2344.htm, last accessed 2019/12/26
12. Standard Test Method for Rockwell Hardness of Plastics and Electrical Insulating Materials, http://mahshahr.aut.ac.ir/lib/exe/fetch.php?media=labs:astm_d785.pdf, last accessed 2019/12/26
13. Wiening, Jonathan (Providence, RI, US), Banta, Marlon (Waltham, MA, US), Endersby, Stephen (Waltham, MA, US) "Predictive Simulation," Patent No. 20160078156. (2016), http://www.freepatentsonline.com/y2016/0078156.html, last accessed 2019/12/26
14. S.M. Sapuan , A. Leenie , M. Harimi , Y.K. Beng , Mechanical properties of woven banana fibre reinforced epoxy composites, Materials and Design 27 (2006) 689–693, Elsevier, (2006).
15. Himanshu Kumar Sinha, Niranjan Thakur, Study on Mechanical Properties of Goat Hair Based Composite, International Journal of Aerospace, Mechanical, Structural and Mechatronics Engineering Vol. 1, Issue. 1, June 2015

IMPRINT

Proceedings of the HSD Student Engineering Conferences

Editors

Prof. Dr.-Ing. Matthias Neef

Prof. Dr.-Ing. M-Sc. Thomas Zielke

Prof. Dr.-Ing. Dipl.-Wirt.-Ing. Jörg Niemann

Dipl.-Kffr. Claudia Fussenecker, M.A.

Faculty of Mechanical and Process Engineering

Hochschule Düsseldorf
University of Applied Sciences
Münsterstraße 156
40476 Düsseldorf

Cover: Elisabeth Steins

DOI: 10.20385/2700-1857/2020.1
URN: urn:nbn:de:hbz:due62-opus-21527

ISSN: 2700-1857